

The Basic Principle of Airyscanning



We make it visible.

The Basic Principle of Airyscanning

Author: Klaus Weisshart

Date: July 2014

Airyscanning is a technique based on confocal laser scanning microscopy. We introduce a detector concept that drastically improves signal by utilizing light that otherwise is rejected by the confocal pinhole. The increased signal-to-noise ratio can be used to retrieve high resolution information. Since this technique uses the confocal principle, it's important first to understand the resolution of a confocal microscope and how it can be boosted using the concept of pixel reassignment. Then, you need to consider how Airyscan from ZEISS distinguishes itself from pixel reassignment and why it excels alongside other related technologies. This paper concludes with a brief discussion of how the Airyscanning principle is put to work technically as an add-on to ZEISS LSM 880 and compares Airyscan technology to structured illumination microscopy (SIM).

Resolution in a confocal microscope

The resolution of a conventional microscope is restricted by the diffraction nature of light [1]. As a result, a point of infinitesimally small extension will be imaged in the lateral plane as a blurred object, the so-called Airy disk, lateral point spread function (PSF) or impulse response (Fig. 1). For two point self-emitters – for example two fluorophores – the Rayleigh criterion is used to define the lateral and axial resolutions (Box 1) [2]. The distribution of the intensity in the Airy disk or the PSF can be described by a so-called Bessel function (Box 2). For practical reasons its central disk is often approximated by a Gauss function. The axial distribution is, on the other hand, represented by a sinc function. Note that axial resolution is approximately three times worse than lateral resolution.

This discussion concentrates on lateral resolution although the same considerations apply for axial resolution.

The probability that a fluorescent point emitter, excited by a point source of a certain wavelength, will be excited is given, considering the distribution of the light intensity of the illumination PSF. You can have a priori information about the illumination PSF since you can measure its intensity distribution and you know the position of its amplitude (e.g. the scan position of the laser beam). Once excited, the point source will emit light of a higher wavelength due to a Stoke's shift. The emission light distribution can also be described by a Bessel function. For the moment, however, assume you are using an integrated detector that covers the whole field of

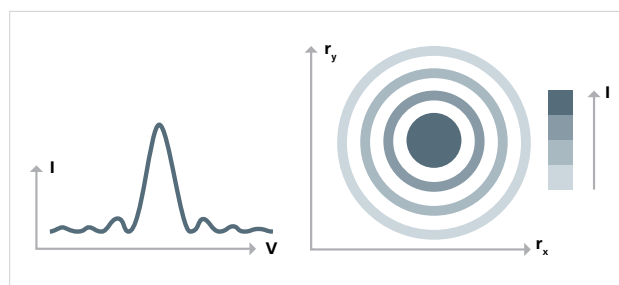


Figure 1 The Airy disk. Given the diffraction nature of light, a point source will be imaged by a microscopic system as a blurred spot surrounded by rings of decreasing intensities (I) in the lateral plane (r_x, r_y) (right panel). The intensity distribution along a transverse direction (v) can be described by a Bessel function (left panel). The first zero point will occur at $1.22 \times \pi$.

view (FOV) and is stationary in regard to the scanned laser beam. In this case, you would not be able to measure the detection PSF; all you would know is that photons have arrived at the detector. Hence, the likelihood of the point emitter being localized at a certain position will be governed exclusively by the excitation PSF (Fig. 2). On the other hand, should you illuminate the whole FOV at a time and use an array detector such as a pixelated camera for detection, the most likely location would be based solely on the detection PSF. Why? Because, when you see a photon, you can then visualize the PSF on the array detector (if the pixels are small enough), but you won't have a clue about the localization of the excitation point source that has caused the photon. This is exactly the situation that exists in classic widefield microscopy.

Now combine point source illumination with array detection, and assume that the detector array stays fixed to the object and the beam is moved. Such a setup is called Image Scanning Microscopy. In this case both the illumination and detection PSF are known. Hence the probability of having a point source at a certain location and simultaneously seeing it at the detector on a discrete site would become the product of the two probabilities or PSFs. As the standard deviation of the product of two probabilities is smaller than the ones from the single probabilities, the effective PSF would narrow and that would increase the precision of the localization estimation (Box 3). Because you are using a point source excitation that is scanned over the FOV, the image points are imaged sequentially. For that very reason you could just as well replace the array detector with an integrating point detector that has a fixed orientation to the point excitation source. If the amplitudes of both the excitation and detection PSFs

are arranged to coincide with the optical axis, so will be the amplitude of their product representing the effective PSF. This type of excitation and detection scheme, in which the object is moved, is used in laser scanning microscopy.

Placing a pinhole to an image conjugated plane will achieve the setup for a classic confocal microscope. Closing the pinhole will narrow the detection PSF and hence raise the contribution of signals with higher localization precisions. The smaller the pinhole becomes, the higher the resolution will be, which scales linear with the pinhole diameter. However, what you gain on resolution by closing the pinhole will reduce detection efficiencies, which scale with the pinhole area, and result in images with poor signal-to-noise ratios (SNR). Therefore it seems not to be too surprising that confocal microscopes are more renowned for their sectioning capabilities as the pinhole rejects out of focus light.

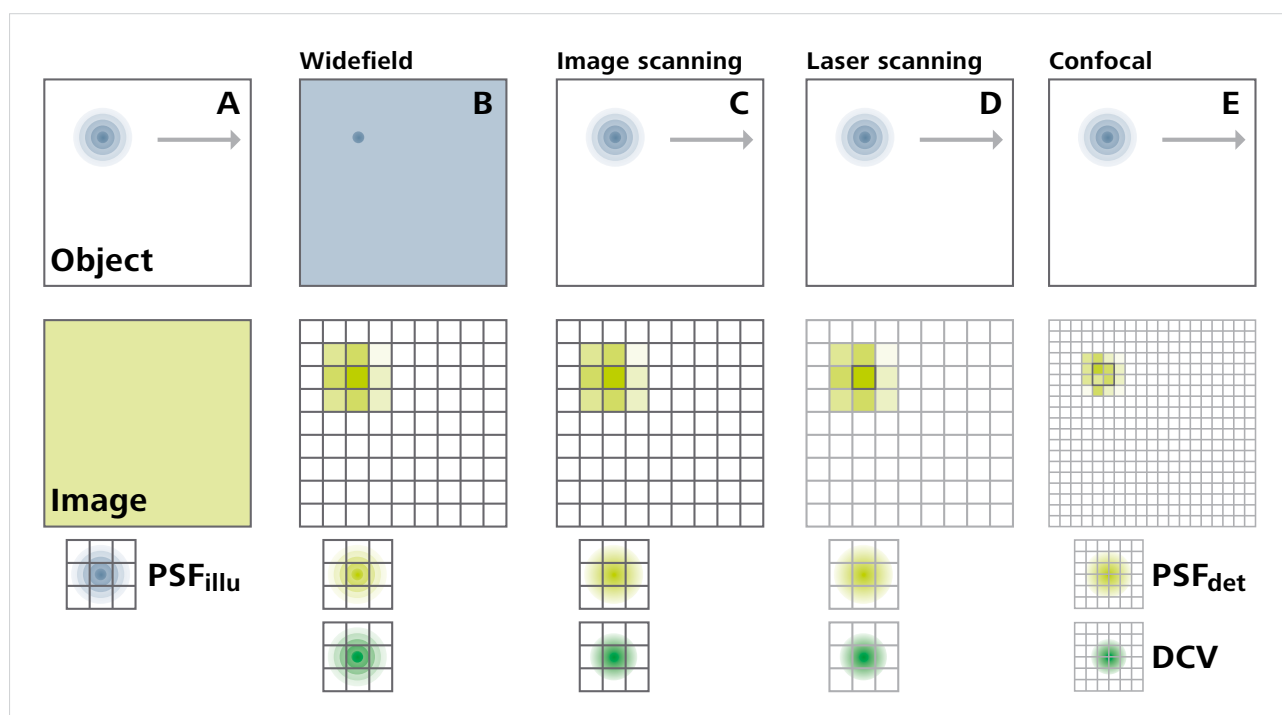


Figure 2 Illumination and detection schemes. The blue dot represents a point emitter, the blue Airy disk the intensity distribution of the illumination laser, the yellow Airy disk the detection PSF, the green Airy disk the deconvolved detection probability. Black square represents a point detector; dark rastered squares an array detector and light rastered squares the area that will be raster scanned. (A) Point source illumination and flat panel detector. (B) Widefield (WF) Microscopy. Widefield illumination and array detector like a camera. (C) Image Scanning Microscopy (ISM). Point source illumination and array detector. The object stays fixed to the detector and the illumination spot is moved in respect to them. (D) Laser Scanning Microscopy (LSM). Point source illumination and integrating point source detector like a photomultiplier tube (PMT) or avalanche photodiode (APD). The illumination spot is fixed to the detector and the object is moved in respect to both. (E) Confocal Laser Scanning Microscopy (CLSM). Point source illumination and integrating pinhole detector.

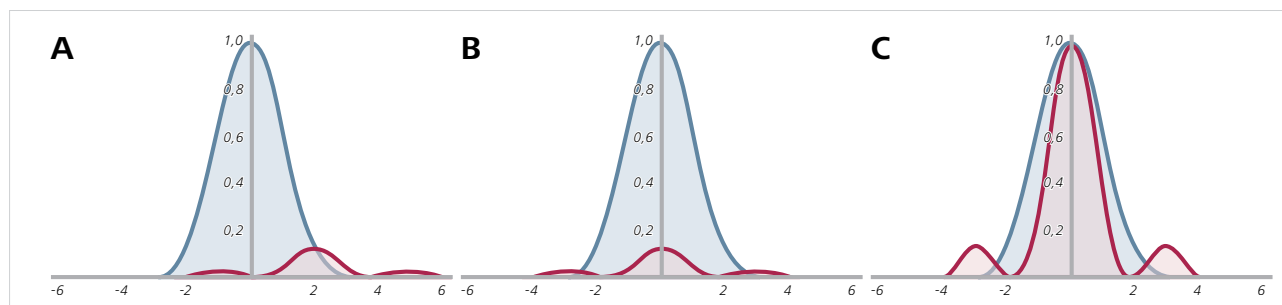


Figure 3 Detector pinhole shift. (A) For a displaced pinhole the effective PSF (red) would be shifted in regard to the PSF from a non-shifted pinhole (blue). Its amplitude and width will be smaller. (B) Since the shift is known, the displaced PSF can be shifted back to the optical axis. (C) Normalized PSFs to show the narrowing of the PSF associated with pinhole shift as well as the increase in the contribution of the side lobes.

For highest resolution gain, the pinhole would have to be closed all the way to zero. It is immediately obvious that this is impractical since light would no longer reach the detector. Therefore, in practical terms, a pinhole diameter of one AU (corresponding to $1.22 \lambda / 2NA$, with λ being the wavelength and NA the numerical aperture of the objective) is used, sacrificing resolution for the sake of SNR. Under these conditions the resolution enhancement is around a factor of 1.4 compared to a widefield system. As confocal images are noisier, deconvolution will be less effective compared to widefield images. This perhaps explains why deconvolution is not very popular for confocal microscopy.

Detector displacement as the base for further resolution enhancement

As seen before, limitations in the SNR prevent to achieve the maximum possible resolution in a confocal microscope. But consider what would happen if the detection pinhole were displaced in regard to the optical axis or the illumination beam [3]. Again, being a product of the illumination and detection PSFs (Fig. 3), the effective PSF would narrow. As the overlap decreases with larger displacements, the width of the resulting Airy disk gets even slightly narrower concomitant with smaller amplitudes (Box 4). In other words, if you see an emitter being excited with a displaced pinhole, the highest probability of its location is within the narrow overlap between the illumination and detection PSFs and consequently it can be localized with higher precision. What is captured with a displaced pinhole contains therefore a higher proportion of higher frequencies. However, you will also get significantly less signal when detecting with a displaced pinhole. This occurs because a point source in the center of the excitation PSF will not be optimally detected as

it lies off-center in respect to the emission PSF. And vice versa, a point emitter located at the center of the emission PSF will not be optimally excited as it is located off-center in regard to the excitation PSF (Fig. 4).

Since the exact shift of the effective PSF against the detection PSF measured on the detector is known, you can shift the signal back to the place where it really belongs. Then you can sum up all the signals from all back shifted pinhole positions, resulting in an increased signal (Box 4). This whole process is called pixel reassignment. The sum image not only has better SNR compared to employing just the central pinhole as more light is collected, it is also sharper. The latter effect is caused by the fact that the displaced pinhole images contain disproportionately higher amounts of better localized emitters compared to the image of the non-displaced pinhole. The larger the displacement, the higher the proportion of better localized emitters. However, the decay in signal with larger shifts and the higher contribution of the side lobes set a limit to how far the detection pinhole might be displaced and to the resolution enhancement that can be achieved practically.

The major part in resolution gain in pixel reassignment is contributed by the increase in SNR. Only a very small part can be attributed to the improvement of the confocal resolution. In addition, the increase in SNR enables a much better deconvolution step that has to follow the pixel reassignment. A deconvolution of a confocal image is less effective for two reasons: the confocal image is noisier and, even with the same SNR, the confocal image lacks the higher frequencies as they are more prone to be obscured by noise.

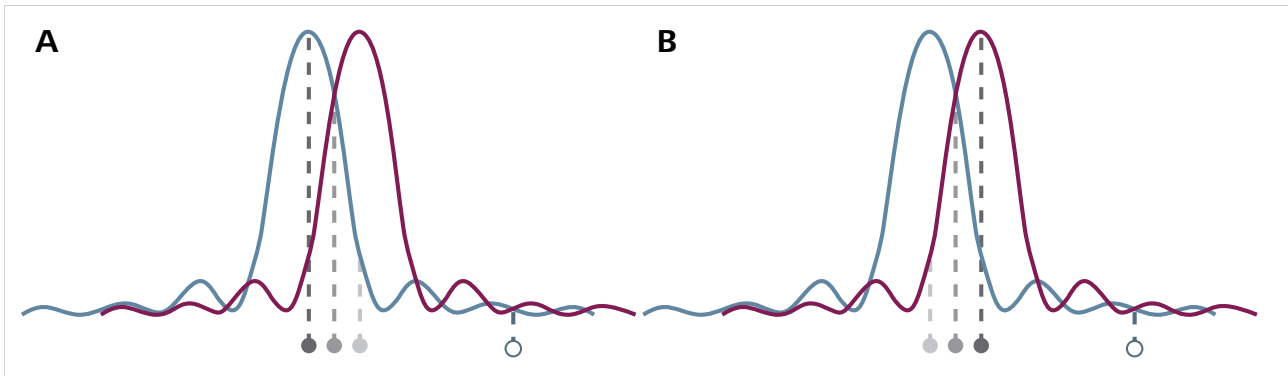


Figure 4 Excitation and detection efficiencies. (A) A point source located on the optical axis (dark grey dot) will be most efficiently excited by the excitation PSF as its intensity is the highest at this position. If the point emitter lies off axis it will be less excited (medium grey and light grey). The higher the offset, the lower the probability it will get excited. If the point emitter lies far off center (open circle), the probability to get excited will approach zero. (B) A point having been excited and emitting photons is best seen if its position overlap the effective PSF amplitude (dark grey spot). With increasing offset position to the detection amplitude it will be less efficiently detected (medium grey and light grey spots). If the point emitter position lies far away from the center (open circle), the likelihood to be detected converge to zero.

One conceptual method of pixel reassignment is to move the pinhole in relation to the optical axis and sum up all the images from one illumination position. But of course this will be slow as an image has to be taken for each displaced pinhole. It's more efficient to replace the pinhole with an array detector at its position. With this setup the distribution of the emitted light is imaged simultaneously for every position of the excitation focus in the sample.

Geometrically in a confocal laser scanning microscope the excitation stays unaltered to the detection as the scanned beam is de-scanned before reaching the detector. Hence the pixel of the array detector that is on the optical axis will always stay on the optical axis and will have the illumination PSF overlapping with the detection PSF. It is instead the object that is moved in relation to the detection, either by a scanning stage with a fixed beam or by scanning the beam with a fixed stage. As other pixels show a displacement to the optical axis, the width of their effective PSFs slightly narrow with increasing displacement. The amplitude of the image intensity decreases and is shifted sideways in the direction of the scan. Finally, another option is to conduct a pixel reassignment followed by a deconvolution step to obtain a higher resolved image. This setup is realized in image scanning microscopy (ISM) using a camera for detection [4]. In a spinning disk microscope this procedure can be parallelized since many pinholes are scanned simultaneously. A technical realization is called multifocal structured illumination microscopy (MSIM) [5].

Pixel reassignment can also be executed straight in the hardware. Because illumination and detection in a confocal microscope are geometrically fixed as the beam is descanned, you can introduce a scan unit in the detection path to re-scan the image. If you choose the sweep factor correctly the detection is shifted by the corresponding amount. In this setup, which is called re-scan confocal microscopy (RCM), the sample will be scanned twice [6]. Yet another possibility is to expand the beam in the pupil plane by a corresponding factor as this will shrink the image on the detector by the same factor. One realization is represented by optical photon reassignment microscopy (OPRA) [7]. The re-scan approach can also be parallelized by simultaneously using multiple excitation spots [8].

In all of these methods based on pixel reassignment, there will be an increase in SNR as light that is otherwise rejected by the pinhole in a confocal microscope will be collected. Aside from SNR, a slighter yet significant contribution to resolution enhancement comes from the effects of narrowing the PSF. The intensities after pixel reassignment are summed up before deconvolution so this information about light contribution from out-of-focus is lost. Therefore the further gain in resolution is limited to the lateral plane. The axial direction stays merely confocal. Methods using cameras are slow because the rate limiting step will be the readout time of this detector. Although these hardware solutions are instant without the need of image processing steps, they lack flexibility as data cannot be manipulated in different ways after acquisition. In addition, they also have lost the axial information and therefore obtain resolution enhancement only in the lateral direction.

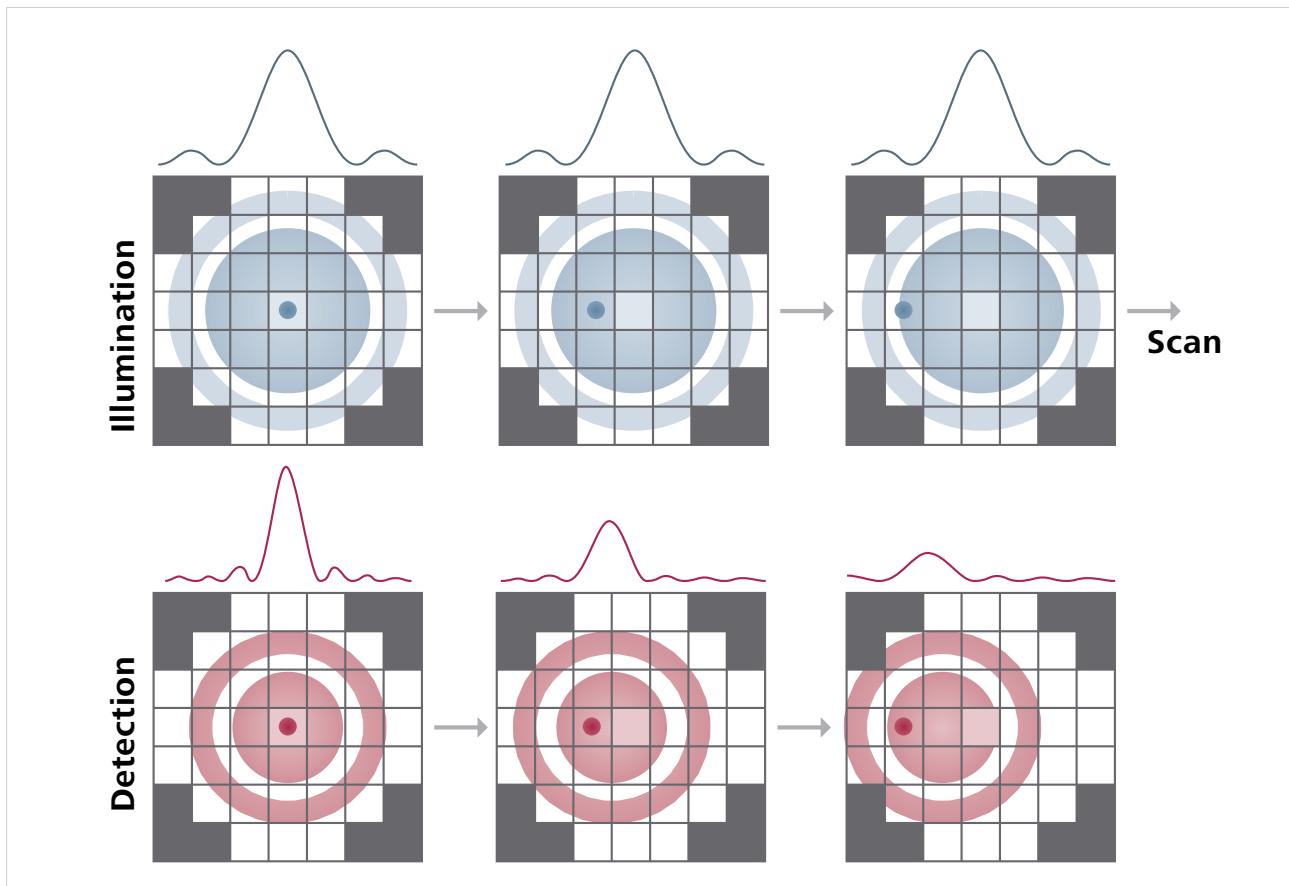


Figure 5 Scanning the Airy disk. A point source (dark dot) located in the object plane is excited by a scanning laser beam to the probability proportional to the intensity distribution of the illumination PSF (blue; upper panel). As each detector element stays fixed to the illumination axis (indicated by the shaded central square), the object will move in relation to the detector as the beam is scanned. In consequence the localization of the point source in the image plane will shift approximately half the distance compared to the displacement of the detector element. The further away a detector element, the smaller will be the amplitude of its effective detection PSF.

The Airyscan principle

Airyscan uses a point detector array as the detector element. This has the advantage of fast readout times and very low dark noise. The central detector element will lie on the optical axis and hence create a classic confocal image on its own. The other detector elements are displaced against the optical axis. Each detector element, if small enough in dimension, can be treated as an individual pinhole. In regard to a point emitter that is imaged, its lateral detection PSF will therefore be scanned (Fig. 5). As the detector elements are displaced from the optical axis, so will be the recorded PSFs of the elements. Therefore each detector element represents a different phase of the image. In consequence, each detector element will record the whole image as the object is scanned. The single recorded images will also be spatially displaced against each other. The larger the displacement of the detector element (or detection PSF) from the optical axis, the narrower the width of the effective PSF will be.

But this effect is only minor and reflects the gain in confocal resolution that is obtained as the contribution of higher frequencies is slightly stronger in the displaced elements. On the other hand, the image intensities will be smaller compared to the central detector. Since the amount of displacement of each detector element is known, you could reassign the measured detection PSFs to the correct position by an appropriate shift, summing all up and performing a deconvolution to obtain an image of increased SNR and resolution in the lateral plane. The gain in SNR contributes the largest part to resolution increase. The resolution in the axial direction would not increase that way and would stay confocal since the out-of-focus information after pixel reassignment would have been lost. Fortunately, there is a more efficient way to analyze the data and this opens the possibility of increasing axial resolution by the same magnitude as lateral resolution.

To understand this approach, you need to consider the image forming process in a confocal microscope (Box 5). The image formed is a convolution of the object with the effective point spread function (PSF) in the spatial domain. In the frequency domain the image will be the product of the object with the optical transfer function (OTF), which is the Fourier transform of the PSF. Therefore deconvolving the image by the effective PSF (or, in frequency domain, the division of the object by the OTF) should be a more appropriate means of restoring the ideal image.

Now, since each detector element acts like a separate pinhole with its own PSF, you can treat the detection PSFs and images of the single elements individually. The detection PSF from each detector element can be multiplied individually with the illumination PSF to obtain the effective PSF of each element (Box 5). By properly weighing the image of each detector element and combining their different positions using the principles of a linear deconvolution, the contribution of each element to the overall signal will be acknowledged. In this way the linear deconvolution step assigns the frequencies to their correct location. This is significantly different from pixel reassignment in which shifting is done before the deconvolution step. Since the information of the axial direction is taken into account by the linear deconvolution step, this produces a resolution enhancement not only in the lateral direction, but also by the same factor in the axial direction. As computation is instant the resolution enhanced image can be displayed in real time. The linear deconvolution performed in the frequency domain acts like a spatial unmixing in the spatial domain, but is mathematically easier to perform (Box 6).

Airyscan add-on to ZEISS LSM 880

Airyscan is a specialized detector tailored for a laser scanning microscope. It is attached to the DC-outport of LSM 880. It is an array of 32 sensitive GaAsP detector elements, arranged in a compound eye fashion. Zoom optics image one up to four Airy units (AU) on the detector diameter (Fig. 6). As the diameter is composed of a maximum of 6 detector elements, each will if 1.25 AU is selected represent a sub-Airy pinhole of approximately $1.25 \text{ AU}/6 = 0.2 \text{ AU}$. In terms of signal a confocal microscope with the pinhole set to 0.2 AU will see less than 5% of the light compared to Airyscan. Emission filters in front of the detector allow you to select the emission light spectrally. GaAsP PMTs distinguish themselves

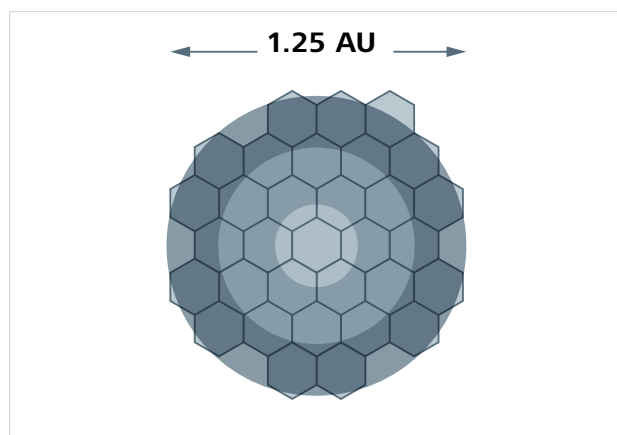


Figure 6 Detector arrangement. 32 GaAsP detector elements are arranged in a compound eye fashion. The central element is adjusted to lie on the optical axis. Other elements group around with increasing distances. For higher resolution applications zoom optics image 1.25 Airy units (AU) onto the detector. The Airy disk intensity distribution (blue) is imaged on the detector elements.

by possessing an excellent quantum efficiency (QE) and extreme low dark counts. Each specific detector in the linear array represents a single pinhole and its displacement from the optical axis. They will record different phases of the image. The displacement of the detection PSFs to the excitation PSF can be used for a more precise localization of point emitters, whereby the excitation PSF is scanned over the image with a fixed geometry between excitation PSF and detector elements. In other words, the detection is fixed in regard to the excitation and it is the object that is moved in regard to both. In this way not only is the image scanned but the Airy disk is also scanned on top.

Fluorescence microscopy is limited by the number of photons that can be collected from a minimal volume in a minimal amount of time. Thus there will always be a compromise between sensitivity, speed and resolution as symbolized by the eternal triangle of compromise [9]. You can improve on all three for a given hardware setting by raising the illumination power. However, this works only to a limited extent as there will be a limited number of photons per fluorophore due to photobleaching and a limited photon flux due to excitation saturation. In addition, phototoxicity induced by high illumination powers is prohibitive in live cell imaging. On the other hand, you can also improve by more efficient light detection. For example, using more sensitive detectors will improve SNR, which can be dedicated to increase sensitivity, speed or resolution. In Airyscan this

improvement is represented by the new detector element. As no light is rejected by a closed pinhole, more photons are collected compared to a conventional confocal and this will significantly increase SNR.

The improved SNR will provide sufficient information for a total improvement in resolution by a factor of 1.7 in all spatial directions. This means that you can achieve a resolution of 140 nm laterally and 400 nm axially for 480 nm. In principle,

as a sub-Airy detector element is in the size of 0.2 AU, the resolution of Airyscan would correspond to a conventional confocal with the pinhole set to 0.2, but with much higher SNR. To achieve a certain resolution, you will have to scan twice as fine. Higher resolution can also be obtained through a virtual NA effect. A 20x / NA 0.8 objective in Airyscan will yield a performance comparable to a 63x / NA 1.4 objective employed in a conventional confocal.

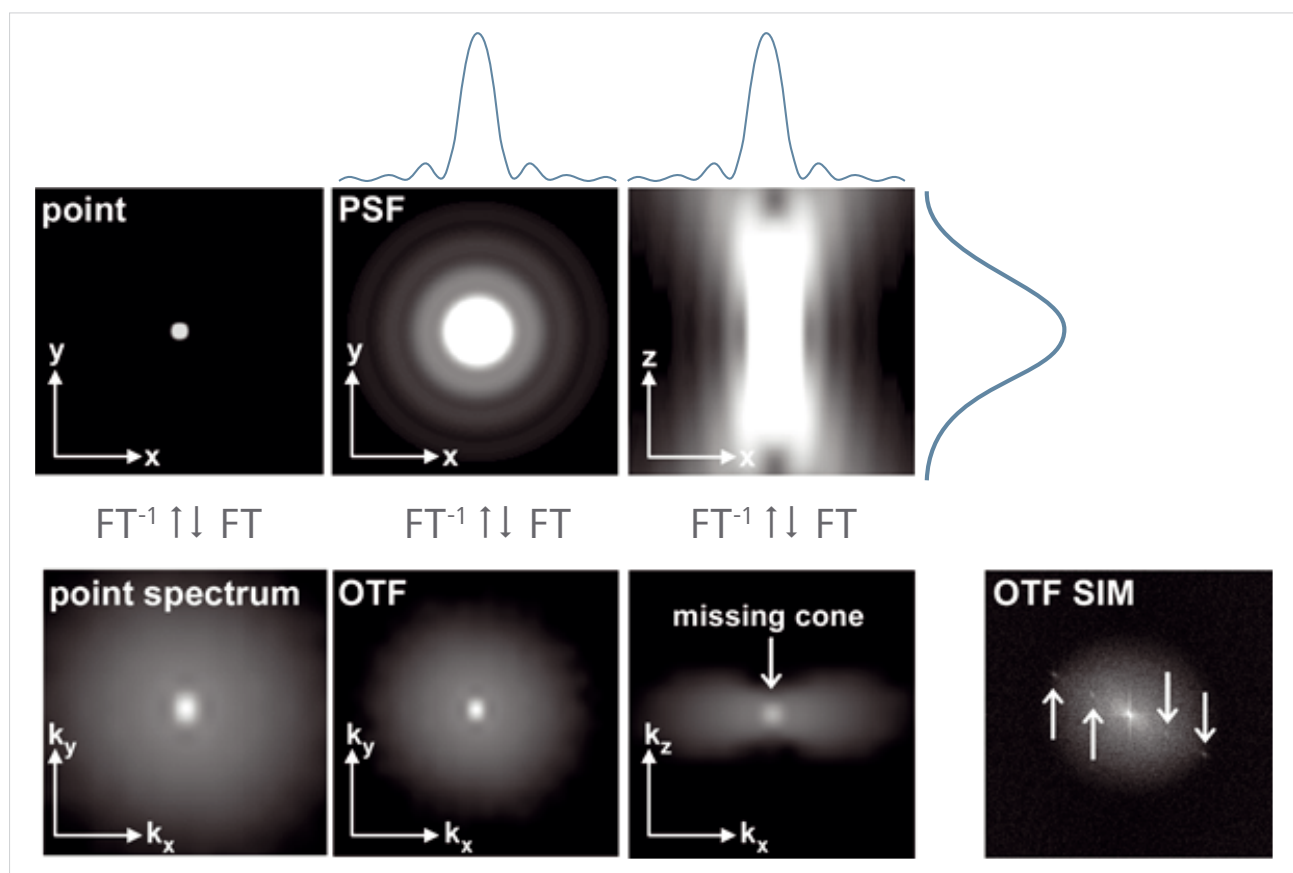


Figure 7 Structuring by the PSF. A point in the xy -plane of the spatial domain will have a wide point spectrum of frequencies. The PSF, of which the lateral intensity distribution is a Bessel function, convolutes the signal leading to a blurred spot in the x,y -plane. An even higher blur occurs in the z -direction, the intensity of which is represented by a sinc function. The OTF, the Fourier transform (FT) of the PSF, on the other hand supports in the k_x,k_y -plane only frequencies up to the cut-off frequency. In the k_z -direction there will be at the zero frequency no support, leading to what is called the missing cone. Whereas the OTF of an imaged point contains all frequencies, the OTF of a grid in SIM contains discrete high frequencies (arrows in the OTF SIM panel) to which frequencies from the interference with object structures are attached. Their orientation is in the direction of the grid. They have two frequencies: either the grid frequency originating from the interference of the 0^{th} order beam with the $\pm 1^{\text{st}}$ order beams of the illumination; or twice the grid frequency, which is caused by the interference of the $+1^{\text{st}}$ and -1^{st} order beams. The zero frequencies are centrally located.

Airyscan compared to structured illumination microscopy (SIM)

In principle, you can think of a confocal microscope as a special case of structured illumination in which the excitation point spread function (PSF) itself represents the structure. This is because the PSF has a defined shape in all directions. In SIM the detector camera and the object are fixed to each other and the illumination is moved by phase steps and rotations. The phases needed in structured illumination are represented in Airyscan, where illumination is fixed to the array detector and the object is moving relative to them, by the displaced detector elements and the scanning steps. A rotation is not necessary because the Airy disk is symmetrical. Likewise, in a spinning disk microscope the pinhole array can be regarded as similar to a grating structure.

While the light in the excitation spot of Airyscan is coherent, the light forming the “point grid” is not: each pixel is illuminated at a different time point (Box 8) so illumination will be incoherent as regards structuring. This is a major difference from SIM, where you have coherent widefield illumination with modulated light that, for example, can be created by a sinusoidal grid pattern projected in the image plane. By way of a three beam interference, discrete high frequencies are generated in the image that can be shifted with their attached frequencies to their correct position (Fig. 7). In Airyscan, on the other hand, the OTF contains no distinct frequencies but all frequencies up to the cut-off frequency. Higher frequencies might be hidden in the noise floor but are more pronounced in the shifted detector elements.

For samples providing high contrast SIM can use all the advantages of a widefield system. It will have the better SNR on its side and as image acquisition is highly parallelized faster frame rates can be achieved. Structured illumination by fringe projection will give a better resolution in these cases because the response at high spatial frequencies is higher (Fig. 8, Box 9). In Airyscan the whole signal on the detector array is

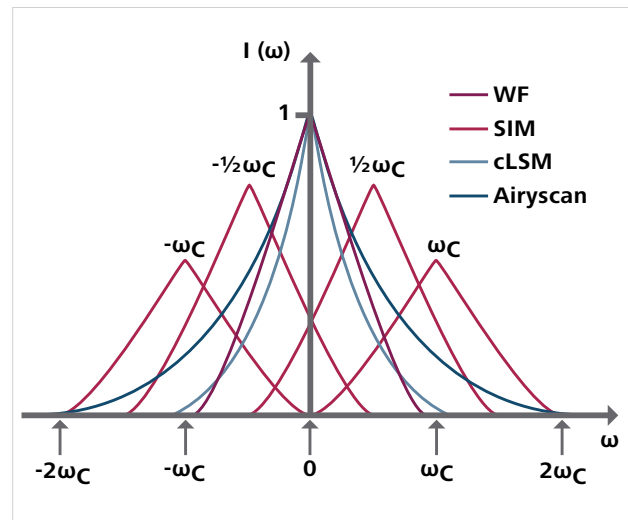


Figure 8 OTF amplitude $I(\omega)$, corresponding to the absolute value of the modulation transfer function (MTF), in widefield (WF, light red), structured illumination microscopy (SIM, dark red), confocal laser scanning microscopy (CLSM, light blue) and Airyscan (dark blue). The OTF of CLSM will have higher frequency contributions than the one for WF. In Airyscan, the OTF will be raised for higher frequencies up to $2\omega_c$ compared to CLSM. In SIM discrete high frequencies at $\pm\omega_c/2$ (grid frequency generated by interference of 0^{th} -order beam with $\pm 1^{\text{st}}$ -order beams) and $\pm\omega_c$ (double grid frequency generated by interference of $\pm 1^{\text{st}}$ -order beams with each other) are generated. The frequency band associated with the ω_c (cut-off) frequency shifted to its appropriate position will extend the captured frequencies by 2 fold ($2\omega_c$). In this way, the proportion of higher frequencies is higher in SIM compared to Airyscan.

detected and will contribute to higher frequencies [10]. As these are not distinct frequencies like in SIM, the OTF expands also to twice the cut-off frequency, but higher frequencies contribute less than in SIM. However, when it comes to thick samples with a significant contribution of out-of-focus light, Airyscan is able to play to its strengths, as the confocal detector elements' pinholes will select light from the focal plane. In SIM out-of-focus light will lead to a decay in the modulation contrast, making this kind of samples problematic to image. In other words, each of the two imaging modalities has its unique strength: Airyscan and SIM are useful complementary technologies.

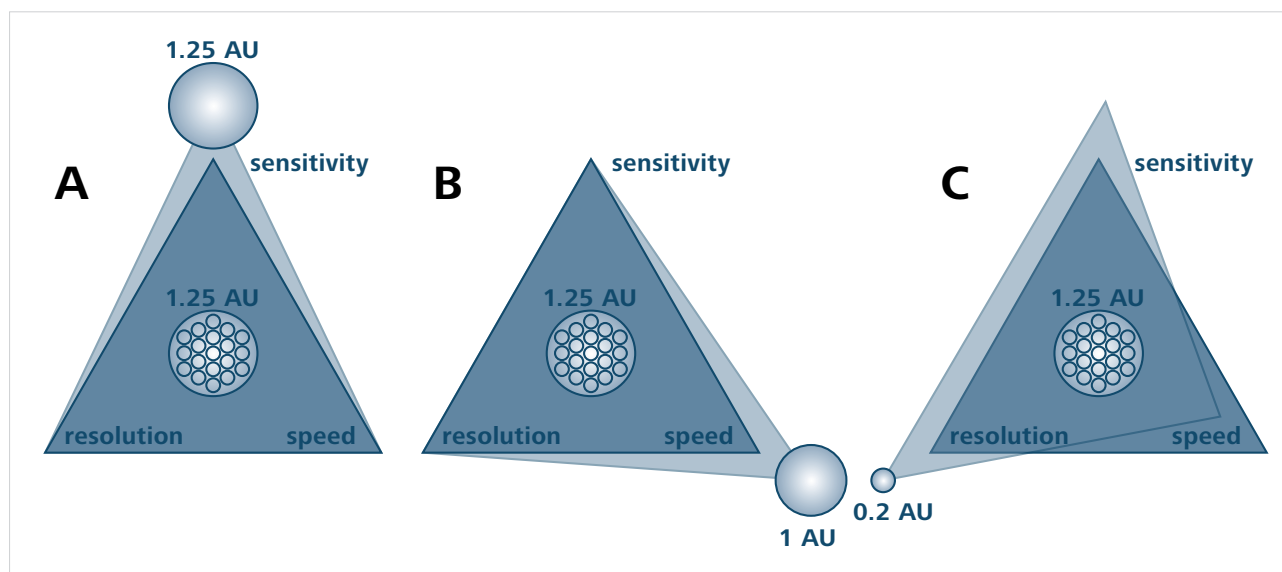


Figure 9 Improving the performance of a confocal laser scanning microscope. By collecting light more efficiently due to its detector array design Airyscan can divert the extra of the photon budget to improve SNR (with the same speed and resolution), speed (with the same SNR and resolution) or resolution (with a reduced speed needed for Nyquist oversampling, but with an improved SNR) as exemplified on the eternal triangle of compromise. (A) For the same SNR and scanning speed, the pinhole in the confocal would have to be opened to 1.25 AU, which would result in loss of resolution. (B) For the same resolution and SNR at a pinhole setting of 1 AU significant averaging of the signal is required in the confocal, which will necessitate a reduction in scanning speed. (C) For the same resolution the pinhole in the confocal would have to be closed to 0.2 AU, which will result in a significant decrease in the SNR. As according to Nyquist criterion you have to sample approximately twice as fine in both the x and y directions, acquisition times will be 4 times slower. Legend: The dark shaded triangle represents the eternal triangle with its corners sensitivity, resolution and speed. The light shaded triangles represent the expansion of these corners. Pinhole sizes for the confocal (open circles) and Airyscan (hexagonal array of small circles within a large circle) are drawn to scale and indicated. The grey shading underlying the pinholes represent the amount of light that is captured.

Summary and outlook

Airyscan is a new confocal detector scheme that allows to efficiently collect light that would be rejected by the pinhole in a standard confocal laser scanning microscope (Fig. 9). This extra photon budget can be diverted to improve sensitivity, speed or resolution. Airyscan consists of a detector array of 32 elements that are arranged in a compound eye fashion providing high flexibility for the imaging mode. First, Airyscan can be used in “standard mode”, where signals collected by individual detector elements are summed up and Airyscan functions as a standard GaAsP detector with resolution governed by the physical pinhole of the LSM 880. Second, it can be set to run in a “virtual pinhole mode” where 4 AU are imaged on the detector array [11]. Post-acquisition one can select and bin

the appropriate detector elements to obtain images between 1 and 4 AU and in this way can trade sensitivity for resolution and vice versa. Third, one can image 1.25 AU on the detector array and by proper oversampling run the detector in a “superresolution (SR) mode”. In this mode a resolution enhancement in all spatial directions by a factor of 1.7 is possible.

In addition, a “virtual NA” effect is achieved. This means that an objective with an NA of 0.8 will provide an SNR comparable to an objective with an NA of $0.8 \times 1.7 = 1.36$.

In essence, Airyscan offers many benefits by expanding the power of a confocal laser scanning microscope.

Literature

1. Abbe, E., *Beiträge zur Theorie des Mikroskops und der mikroskopischen Wahrnehmung*. Archiv Mikroskop Anat, 1873. 9: p. 413-468.
2. Born, M. and E. Wolf, *Principles of Optics: Electromagnetic Theory of Propagation, Interference and Diffraction of Light*. 7 ed. 1999, Cambridge, New York, Melbourne, Madrid, Cape Town: Cambridge University Press.
3. Sheppard, C.J., S.B. Mehta, and R. Heintzmann, *Super-resolution by image scanning microscopy using pixel re-assignment*. Opt Lett, 2013. 38(15): p. 2889-2892.
4. Muller, C.B. and J. Enderlein, *Image scanning microscopy*. Phys Rev Lett, 2010. 104(19): p. 198101.
5. York, A.G., et al., *Resolution doubling in live, multicellular organisms via multifocal structured illumination microscopy*. Nat Methods, 2012. 9(7): p. 749-754.
6. De Luca, G.M., et al., *Re-scan confocal microscopy: scanning twice for better resolution*. Biomed Opt Express, 2013. 4(11): p. 2644-2656.
7. Roth, S., et al., *Optical photon reassignment microscopy (OPRA)*. Optical Nanoscopy, 2013. 2(5): p. 1-6.
8. York, A.G., et al., *Instant super-resolution imaging in live cells and embryos via analog image processing*. Nat Methods, 2013. 10(11): p. 1122-1126.
9. Shotton, D.M., *Robert Feulgen Prize Lecture 1995. Electronic light microscopy: present capabilities and future prospects*. Histochem Cell Biol, 1995. 104(2): p. 97-137.
10. Barth, M. and E. Stelzer, *Boosting the optical transfer function with a spatially resolving detector in a high numerical aperture confocal reflection microscope*. Optik, 1994. 96(2): p. 53-58.
11. Pawley, J.B., M.M. Blouke, and J.R. Janesick. *CCDiode: an optimal detector for laser confocal microscopes*. in *Electronic Imaging: Science & Technology*. 1996. International Society for Optics and Photonics.

Box 1: Rayleigh criterion

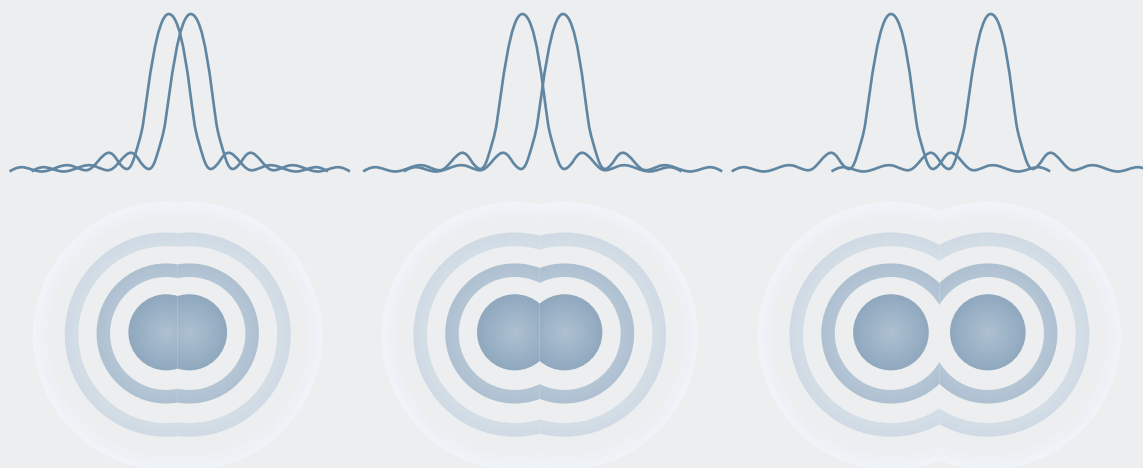


Figure B1 Airy diffraction pattern generated by two point sources. Points closer than the Rayleigh criterion (left) are difficult to distinguish whereas points meeting the Rayleigh criterion (middle) or far apart (right) can be separated.

The Rayleigh criterion defines the minimal distance two point self-emitters must maintain to identify them still as separate entities in fluorescence microscopy. This minimum distance is equal to the distance of the first minimum from the center of the Airy disk. In other words, two point light sources are considered to be resolved, when the diffraction maximum of one imaged point coincides with the first minimum of the other. If the distance exceeds the minimum, the two point sources are well resolved. If the distance falls under this limit, they are regarded as not resolved.

As the intensity distribution of the Airy disk (lateral PSF) is described by a Bessel function, the first minimum is at a distance 1.22π , from which the minimum lateral distance (d_{lat}) can be computed (equation 1). Similar considerations using a sinc function for the axial direction can be used to retrieve the minimum axial distance d_{ax} (equation 2).

$$(1) \quad d_{lat} = \frac{1.22 \cdot \lambda}{2 \cdot NA} = \frac{0.61 \cdot \lambda}{NA} = \frac{0.61 \cdot \lambda}{n \cdot \sin \alpha}$$

$$(2) \quad d_{ax} = \frac{2 \cdot n \cdot \lambda}{NA^2}$$

The minimum distance "d" is defined in the spatial domain. In the frequency domain, this would correspond to a maximum frequency "f" the system can transmit. As "f" is inverse to "d", the cut-off frequencies in the lateral (equation 3) and axial (equation 4) directions can be computed.

$$(3) \quad f_{lat} = \frac{NA}{0.61 \cdot \lambda}$$

$$(4) \quad f_{ax} = \frac{NA^2}{2 \cdot n \cdot \lambda}$$

Parameters: d : minimal distance, f : cut-off frequency, NA : numeric aperture of objective, n : refractive index of medium, λ : wavelength, α : half opening angle of objective

Another popular approach to define resolution is the Houston criterion. Resolution is hereby defined as the full width at half maximum (FWHM) (equations 5 and 6).

$$(5) \quad FWHM_{lat} = \frac{0.51 \cdot \lambda}{NA}$$

$$(6) \quad FWHM_{ax} = \frac{1.77 \cdot n \cdot \lambda}{NA^2}$$

Box 2: Intensity distribution of the point spread function (PSF)

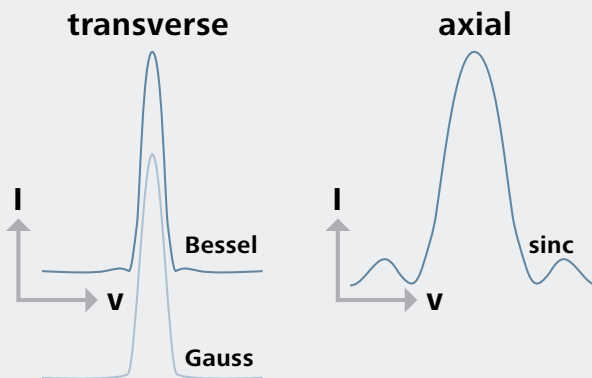


Figure B2 Intensity distributions in the point spread function. The transverse intensity distribution is based on a Bessel function, which can be approximated by a Gauss function (left). The axial intensity distribution can be described by a sinc function (right). Simulated parameters: I_0 : 1, NA: 1.44, λ : 525 nm, n : 1, r_0 : 0, z_0 : 0; amplitudes have been normalized.

The transverse intensity distribution of the lateral point spread function (PSF) or the Airy disk of a fluorescent pointemitter is described by a Bessel function of 1st order and 1st kind (equation 1). The central disc can be approximated by a Gaussian function (equation 2). In the axial direction, the intensity distribution is given by a sinc function (equation 3). There is not a good Gauss representation for the axial direction.

$$(1a) \quad I(r) = I_0 \cdot \left(\frac{2 \cdot J_1(v)}{v} \right)^2$$

$$(1b) \quad v = \frac{2 \cdot \pi \cdot NA \cdot (r - r_0)}{\lambda}$$

$$(2a) \quad I(r) = I_0 \cdot e^{-\frac{(r - r_0)^2}{2 \cdot \sigma^2}}$$

$$(2b) \quad \sigma = \frac{0.42 \cdot \lambda}{2 \cdot NA}$$

$$(3a) \quad I(r) = I_0 \cdot \left(\frac{\sin \frac{v}{4}}{\frac{v}{4}} \right)^2$$

$$(3b) \quad v = \frac{2 \cdot \pi \cdot NA^2 \cdot (z - z_0)}{\lambda \cdot n}$$

I_0 : amplitude

J_1 : Bessel function of 1st order and 1st kind

NA: numerical aperture of objective lens

λ : wavelength of light

n : refractive index of medium

r : transverse distance

r_0 : transverse center

z : axial distance

z_0 : axial center

Box 3: Effective PSF in a confocal system

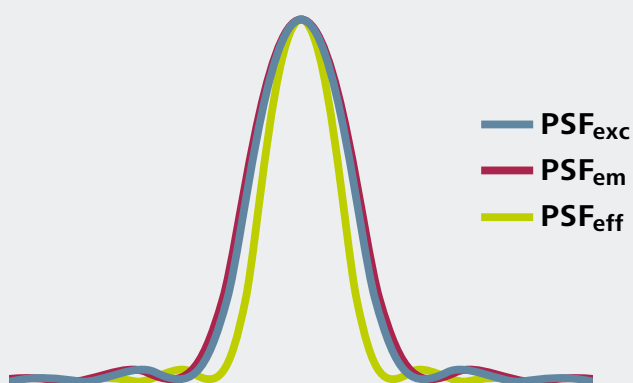


Figure B3 Product of two Bessel functions. The product of the excitation PSF (PSF_{exc}) and emission PSF (PSF_{em}) will yield an effective PSF (PSF_{eff}) with reduced width. Please note that the detection PSF (PSF_{det}) will be equal to PSF_{em} in a widefield system. In a confocal it will be the convolution of PSF_{em} with the pinhole (PH). As the laser fiber acts as a pinhole the illumination PSF (PSF_{illu}) equals PSF_{exc} in both cases. Simulated parameters: l_0 : 1, NA: 1.44, λ_{ex} : 488 nm, λ_{em} : 525 nm, n : 1, r_0 : 0; amplitudes have been normalized.

In the spatial domain, the confocal PSF or impulse response is the product of the detection PSF and the illumination PSF (equation 1). The detection PSF equals the emission PSF convolved with the pinhole PH of diameter "d". If the diameter of the pinhole is equal and below 1 AU, the convolved product can still be approximated by a Bessel function. The product of the illumination PSF with the

detection PSF has a narrower width than the single original PSFs. If we approximate the Bessel function by a Gauss function, the width represented by the standard deviation " σ " of the product will be narrowed compared to the widths of the input PSFs (equation 2). Also the transverse location " r_0 " of the amplitude " I_0 " of the product will lie between the locations of the amplitudes of the original functions (equation 3). Of course, if the amplitudes of both illumination and detection PSFs would fall on the optical axis, so would the amplitude of the product. The Fourier transform of the PSF is the optical transfer function (OTF) in the frequency domain. The product in the PSFs in the spatial domain corresponds to a convolution of the OTFs in frequency space (equation 4). The highest resolution in a confocal microscope would be obtained, if the pinhole would be infinitesimally small. Then the pinhole becomes a so called deltafunction equaling 1 and the effective PSF would just be the product of excitation and emission PSF. This would yield the highest possible resolution of the confocal microscope, but at the cost of SNR. Of course a completely closed pinhole is prohibitive to imaging, as no light could reach the detector. So the theoretical possible resolution of a confocal cannot be reached. For the sake of SNR one compromises to a pinhole size in the range of 1 AU.

$$(1) \quad PSF_{conf}(r) = PSF_{illu}(r) \cdot PSF_{det}(r) = PSF_{exc}(r) \cdot (PSF_{em}(r) \otimes PH(d))$$

$$(2) \quad \sigma_{conf} = \sqrt{\frac{\sigma_{illu}^2 \cdot \sigma_{det}^2}{\sigma_{illu}^2 + \sigma_{det}^2}}$$

$$(3) \quad r_{0,conf} = \frac{r_{0,illu} \cdot \sigma_{det}^2 + r_{0,det} \cdot \sigma_{illu}^2}{\sigma_{illu}^2 + \sigma_{det}^2}$$

$$(4) \quad OTF_{conf}(k_r) = FT(PSF(r)_{illu} \cdot PSF(r)_{det}) = OTF_{illu}(k_r) \otimes OTF_{det}(k_r)$$

Box 4: The principle of pixel reassignment

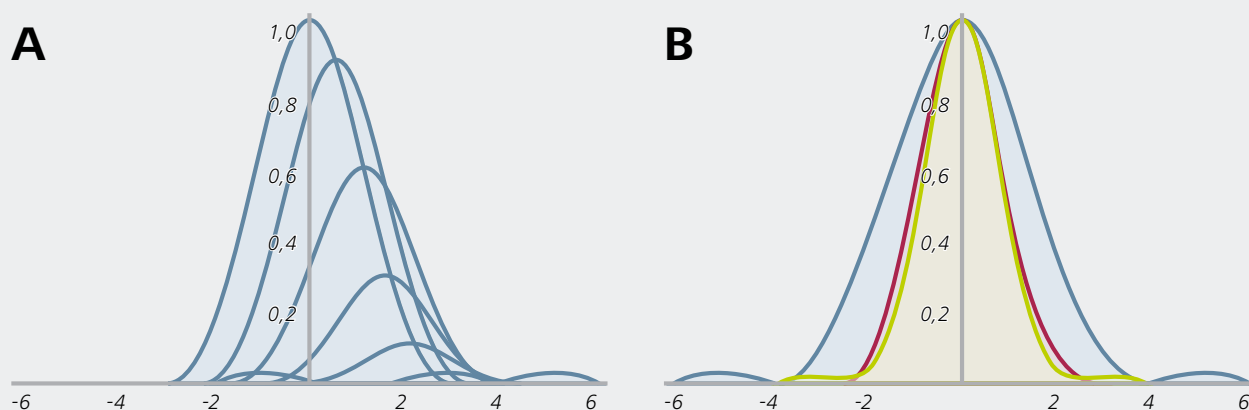


Figure B4 Pixel reassignment. (A) Cross-section through the image of a point object in a scanning microscope for a point detector that is displaced by a normalized distance from the optical axis, if no Stoke's shift occurs. The peak intensity is reduced and shifted sideways as the offset is increased. (B) Reassigned and summed up PSFs from (A) result in a sharper PSF (green) with increased amplitude. The PSF from confocal (red) and widefield (blue) are used for comparison. Amplitudes have been normalized to compare the widths.

Let us assume the pinhole is displaced by a certain distance v_d (as defined in equation 1) away from the optical axis v_0 , which is defined by the scan position or the illumination PSF. For a zero displacement ($v_d=0$) corresponding to a point on the optical axis, one will obtain exactly a confocal image for that pixel as the image is scanned. If the detection pinhole, however, is displaced, the amplitude of the effective PSF will be shifted in the direction of the scan by a certain amount. As it is still the product of two PSFs, it will have a narrower width than is the case for the non-displaced pinhole (see box 3). As the overlap decreases with increasing displacement the width of the effective PSF gets increasingly narrower. If therefore an emitter is seen through the displaced pinhole, the likelihood that it is more precisely localized increases. In other words, higher frequencies are more pronounced in the displaced pinhole image and their proportion rises the further the displacement goes. But as the pinholes get more displaced, the amplitudes will be reduced and the side lobes get more pronounced. So there is a restriction as to the extent one can shift.

Let us see, how big the shift will be in the transverse direction. If the detection PSF is shifted by an amount v_d , the effective PSF will be shifted by a fraction of this amount dependent on the widths of illumination and detection PSFs and their

offset (equation 2). In the situation of no Stokes shift with excitation and emission wavelengths being the same, the factor would be $\frac{1}{2}$. If a Stoke's shift applies, the factor can be calculated from the ratio of the emission to excitation wavelength (equation 3).

Since the shifts of the effective PSFs are known, shifting back the images from the off-axis detectors to v_0 and adding them up, will result in a sharper PSF. This shift and summation is called pixel reassignment.

$$(1) \quad v_d = \frac{2 \cdot \pi \cdot (r_d - r_{0,d}) N A_d}{\lambda_{em}}$$

$$(2) \quad v_0 = a \cdot v_d ; 0 \leq a \leq 1$$

$$(3a) \quad a = \frac{1}{1 + \beta}$$

$$(3b) \quad \beta = \frac{\lambda_{em}}{\lambda_{exc}}$$

Parameters: v_d : normalized transverse position in detector plane, a : scale factor of displacement, r_d : transverse position in detector plane, $r_{0,d}$: offset position from optical axis, β : wavelength ratio, λ_{exc} : excitation wavelength, λ_{em} : emission wavelength

Box 4 continued

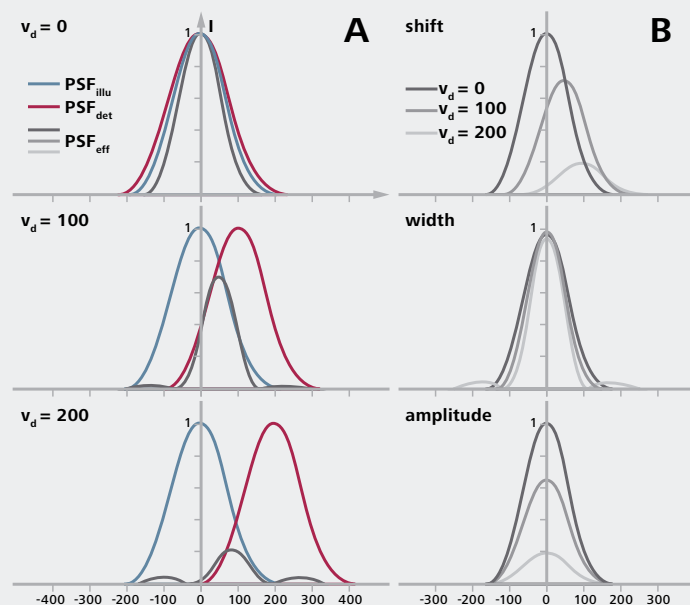


Figure B4c Pixel reassignment. (A) The effective PSF (PSF_{eff} ; grey) as a product of illumination PSF (PSF_{illu} ; blue) with detection PSF (PSF_{det} ; red) at increasing detector displacements v_d (from top to bottom). (B) Shift (upper panel), width (central panel) and amplitude (lower panel) of the effective PSF at different detector displacements v_d .

The effective PSF in a confocal microscope with aligned illumination and detection is the product of the illumination PSF with the detection PSF. It will therefore be narrower. As the detector element is displaced in the transverse direction (v), the amplitude of the detection PSF will be shifted the same way. The resulting effective PSF will shift by a smaller increment (approximately half) and has a decreased amplitude. It will also be slightly narrower and asymmetric compared to the case for the on-axis detector. The narrowing and asymmetry is caused by the side lobes of the Bessel function.

To estimate the shift and the amplitude, we can approximate the central disc by a Gauss function (equation 1). For the sake of simplicity let us look at the normalized form in which the amplitude (I_0) equals 1. Let us further assume that

$$(1) f(x) = \frac{1}{\sqrt{2\pi}\sigma} \cdot e^{-\frac{(x-\mu)^2}{\sigma^2}} = I_0 \cdot e^{-\frac{(x-\mu)^2}{\sigma^2}}$$

$$(2) f_{illu}(x) = f_{det}(x) = e^{-\frac{x^2}{\sigma^2}}$$

$$(3) f_{illu}(x) \cdot f_{det}(x) = e^{-\frac{x^2}{\sigma^2}} \cdot e^{-\frac{x^2}{\sigma^2}} = e^{-\frac{2 \cdot x^2}{\sigma^2}} = e^{-\frac{x^2}{(\sigma/\sqrt{2})^2}}$$

illumination and detection PSF would lie on the optical axis with no displacement ($\mu=0$). Finally if excitation and emission wavelengths are the same, the standard deviation " σ " of the illumination and detection PSFs will also be the same (equation 2). Their product would be another Gauss function that has a width reduced by a factor of square root of 2. If the detection Gauss would have an offset of " a " (equation 4), then the product with the illumination PSF would yield again a Gauss function with a width reduced by a factor of square root 2. Please note, as we only simulate the central disc by the Gauss function without the side lobes, no further narrowing as is the case with Bessel functions, will be observed. The amplitude of that Gauss function will have an offset of " $a/2$ " and an amplitude that is reduced by an exponential scaling factor that becomes smaller with increasing " a ".

$$(4) f_{det,a}(x) = e^{-\frac{(x-a)^2}{\sigma^2}}$$

$$(5) f_{illu}(x) \cdot f_{det,a}(x) = e^{-\frac{x^2}{\sigma^2}} \cdot e^{-\frac{(x-a)^2}{\sigma^2}} = e^{-\frac{a^2}{4}} \cdot e^{-\frac{(x-a/2)^2}{(\sigma/\sqrt{2})^2}}$$

Box 5: Image formation in a confocal microscope



Figure B5 Image formation in a confocal system. The object $O(r)$ in the spatial domain is convolved by the effective PSF $EH(r)$ to obtain the Image $D(r)$, which will be blurred. Additionally, noise added on top of the convolution can contribute to the image (not shown). In the frequency domain, the object spectrum $O(\omega)$ will be multiplied with the effective optical transfer function $EH(\omega)$ to yield the image spectrum $D(\omega)$. Spatial domain and frequency domain can be obtained from one another by Fourier transformation (FT) or reverse Fourier transformation (FT^{-1}).

The image in a confocal system is the result of the convolution of the object by the effective PSF in the spatial domain.

Noise will add to the image. Because each detector element in Airyscan acts as an independent pinhole, the image formed by each detector element will be a convolution of the object by the effective PSF of each element plus added noise. In the frequency domain, the Fourier transform (FT) of the image of

each detector element will be the product of the object spectrum with the effective OTF of the respective detector element plus added noise spectrum (equation 2).

By inference, if the image is deconvolved by the effective PSF, one should be able to reconstitute the true object structures. Likewise, if the image spectrum is divided by the effective OTF, one can obtain the object spectrum that will be inverse Fourier transformed (FT^{-1}) to obtain the true object. To reconstitute the object spectrum one will have to weigh the contribution of each detector element to the image and deconvolve the sum of each detector element. This is handled conveniently by a linear Wiener deconvolution, which takes noise into account (equation 4).

$$(1) \quad D_i(r) = O(r) \otimes EH_i(r) + N(r)$$

$$(2) \quad D_i(\omega) = O(\omega) \cdot EH_i(\omega) + N(\omega)$$

$$(3) \quad O(\omega) = \frac{\sum_i^n (D_i(\omega) \cdot EH_i^*(\omega))}{w + \sum_i^n |EH_i(\omega)|^2}$$

$$(4) \quad w = \frac{\langle |N(\omega)|^2 \rangle}{\langle |O(\omega)|^2 \rangle}$$

Parameters: $O(r)$: object, $D(r)$: image, $N(r)$: noise, $EH(r)$: PSF_{eff} , $O(\omega)$: object spectrum, $D(\omega)$: image spectrum, $N(\omega)$: noise spectrum, $EH(\omega)$: OTF_{eff} , i : index of detector elements, n : number of detector elements, w =Wiener parameter

Box 6: Spatial unmixing

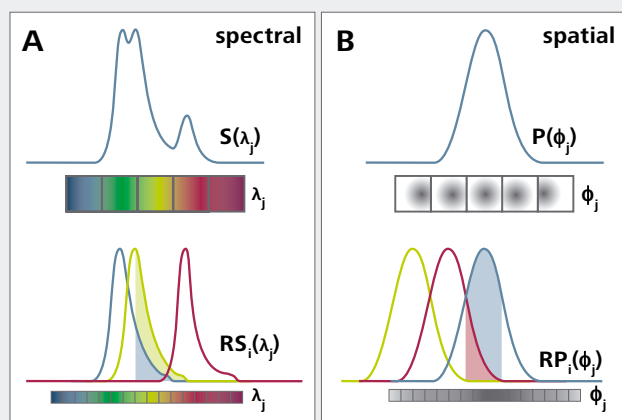


Figure B6 Analogy of spectral and spatial linear unmixing. (A) In spectral unmixing reference spectra $RS_i(\lambda_j)$ of each dye i in spectral channel λ_j can be recorded using pixels of the image with only dye i present (lower panel). The more spectral channels are used, the finer the resolution of the reference spectrum. The example shows 16 channels and the normalized spectra of three dyes (blue, green and red lines). To resolve 3 dyes a minimum of 3 channels would be required; however a 1.5 oversampling is recommended. This would translate to 5 channels ($1.5 \times 3 = 4.5$ rounded up to 5). Dependent on their contribution the three spectra add up per pixel to the measured spectrum $S(\lambda_j)$ (upper panel, violet line). Their contribution to the middle of the 5 spectral channels is depicted by the shaded areas underneath the spectral curve. As the total spectrum is measured and the reference spectra are known, the proportion of each dye contributing to the total spectra can be calculated. (B) In spatial unmixing reference PSFs $RP_i(\phi_j)$ are recorded in phase channels ϕ_j generated by displaced sub-pixel detection elements. From their displacement from the optical axis the shift of the reference PSF amplitudes can be calculated. The more phase channels are used, the finer will be the potential resolution (lower panel). The example shows 16 channels and the normalized PSFs from 3 of the detector elements (blue, green and red lines). To obtain better resolution a minimum of 2 channels is required. However, as overestimation minimizes the error 5 phase channels are considered (upper panel). Dependent on their contribution the three PSFs add up per pixel to the measured PSF $P(\phi_j)$ (violet line). Their contribution to the central detection element is depicted by the shaded areas beneath the PSFs. As the total PSF is measured and the displacement of the reference PSFs are known by computation, one can calculate the weight of the single detector elements to the measured PSF.

In spectral unmixing each pixel contains as a spectrum the weighted sum of all present spectra (equation 1). The proportions of each component can be retrieved by solving the linear system of equations. The solution can be obtained using an inverse least squares fitting approach that minimizes the square difference between the measured and calculated spectra. If number of components (i) equals the number of channels (j), that is $i=j$, then the least square analysis will equal "0"; otherwise if $j > i$ (overestimated system) the solution of the differential equations approaches a minimum value.

$$(1) \quad S(\lambda_j) = \sum_i a_i \cdot RS_i(\lambda_j)$$

$$(2) \quad \frac{\partial \sum_j [S(\lambda_j) - \sum_i a_i \cdot RS_i(\lambda_j)]^2}{\partial a_i} \rightarrow \min$$

Parameters: $S(\lambda_j)$: spectrum in spectral channel λ_j , $RS_i(\lambda_j)$: reference spectrum of component i in channel λ_j , a_i : weight (proportion) of component i , i : index of component, j : index of channel

In spatial unmixing each pixel contains a spectrum of the weighted sum of the signal of all detector elements (equation 3). The contribution of each element can be retrieved by solving the linear equation system. The solution can be obtained using an inverse least squares fitting (equation 4).

$$(3) \quad P(\phi_j) = \sum_i a_i \cdot RP_i(\phi_j)$$

$$(4) \quad \frac{\partial \sum_j [P(\phi_j) - \sum_i a_i \cdot RP_i(\phi_j)]^2}{\partial a_i} \rightarrow \min$$

Parameters: $P(\phi_j)$: PSF displacement in channel ϕ_j , $RP_i(\lambda_j)$: reference PSF displacement of component i in channel ϕ_j , a_i : weight (proportion) of component i , i : index of component, j : index of channel

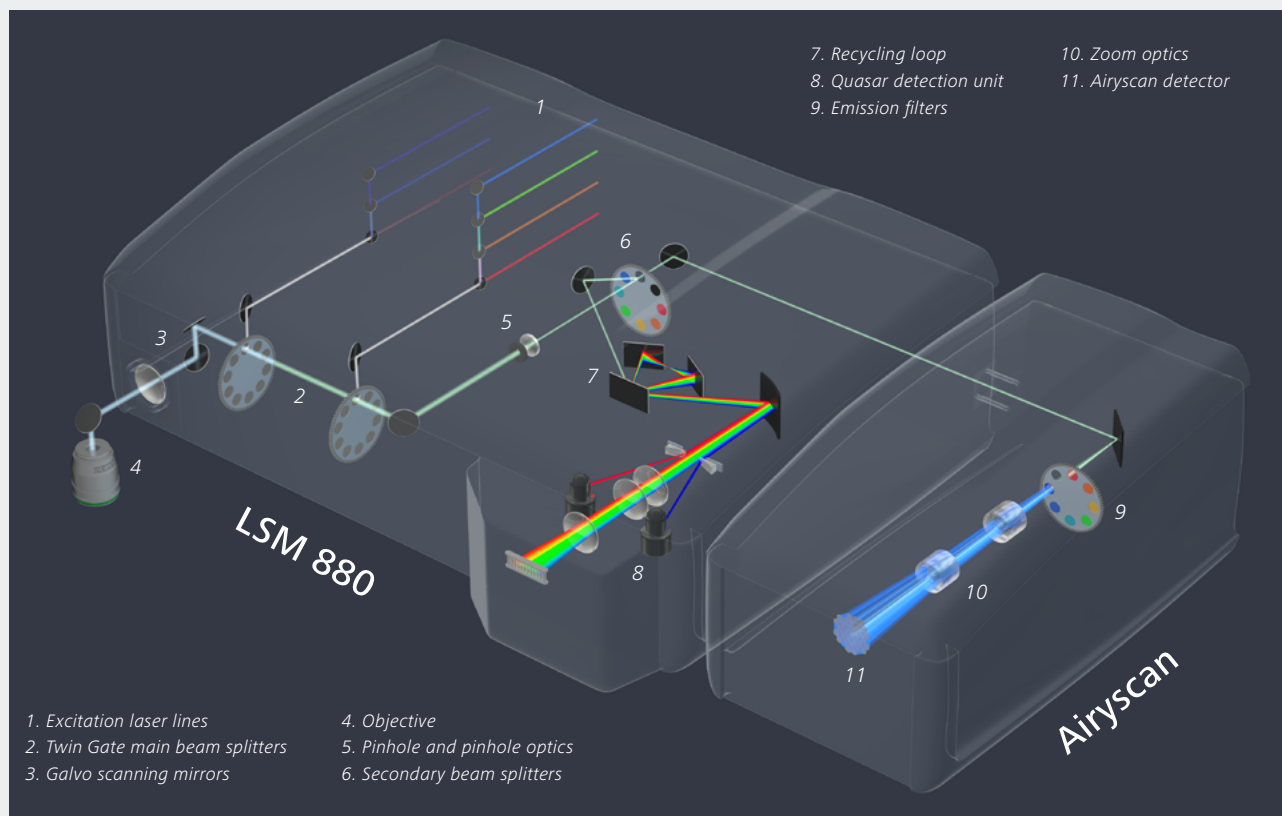
Box 7: LSM 880 with Airyscan

Figure B7 The Airyscan unit attached to the Zeiss LSM 880.

What is Airyscan?

Airyscan is a special detector module added to the out coupling port of LSM 880. Its design enables to be more light efficient than would be possible with a standard confocal point detector. The extra on photons can be used to increase the sensitivity of the image, to scan faster or to improve the resolution.

What is the principle of the Airyscan detector?

The Airyscan detector consists of a Gallium Arsenide Phosphid (GaAsP) photomultiplier tube (PMT) array of 32 elements, which are arranged in a compound eye fashion. In this way each detector element receives light that is displaced from the optical axis by defined distances.

How efficient is the Airyscan detector?

The GaAsP detector is ideal for confocal laser scanning microscopy due to its high quantum efficiency (QE), extreme low dark counts and fast read out times.

What is the resolution gain in Airyscan?

A resolution gain of 1.7 fold is obtained in all spatial directions.

How is the resolution increased by Airyscan?

The majority of resolution improvement stems from the significant increase in SNR. In the superresolution (SR) mode 1.25 Airy units (AU) will be imaged on the detector array. Since along the diagonal there is a maximum of 6 elements, each of them acts as a pinhole of $1.25 \text{ AU} / 6 \approx 0.2 \text{ AU}$. In other words, one obtains a resolution comparable to a confocal microscope with the pinhole set to 0.2 AU, but with a much better SNR. A pinhole set to 0.2 AU in a standard confocal will capture only 5% of the light compared to Airyscan.

What is the advantage of Airyscan compared to other technologies based on pixel reassignment?

First of all, a resolution gain in Airyscan is obtained for all lateral and axial directions. All other methods show only lateral resolution gain; axial resolution will stay confocal. Second, compared to hardware solutions, you have all the flexibility to analyze data post acquisition in different ways.

Box 8: Structuring the Object

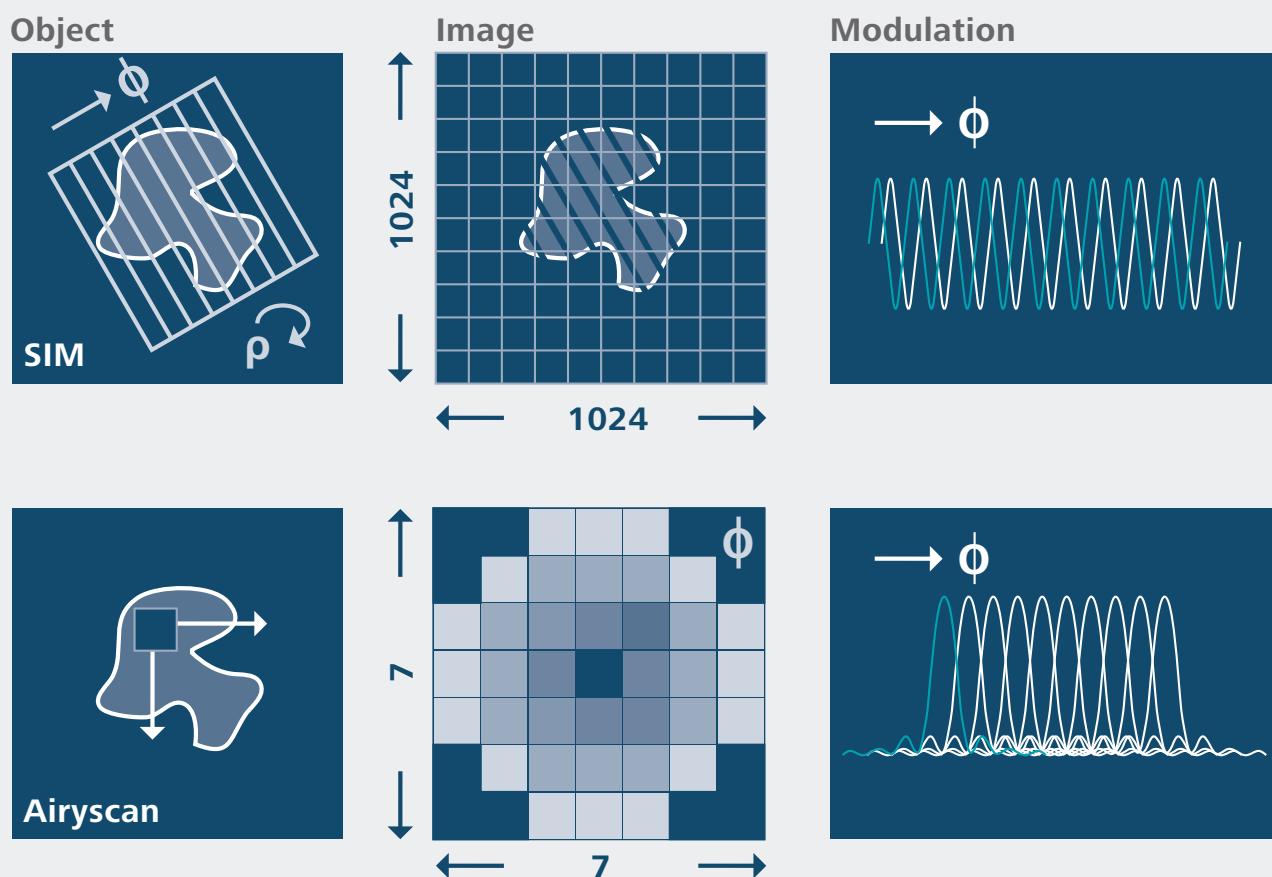


Figure B8 Structuring the object in SIM and Airyscan. In Structured illumination (SIM) (upper panel) the object is modulated by for example a sinusoidal pattern. The pattern is shifted laterally (ϕ) (5 times) to create necessary phases for the deconvolution step and rotated (ρ) (3 times) to get isotropic coverage of the sample. The image will contain the object as well as the grid pattern generated by interference of the diffracted excitation light. As widefield illumination is used the whole sample for each phase is imaged on the pixelated camera (1024 x 1024 pixel in the example). In Airyscan (lower panel) the sample is illuminated by a point source so only a small portion of the object is excited. The object is imaged on a point array detector. Each of the detector elements will image the point of excitation. As they are displaced to different amounts in regard to the optical axis the images created by scanning the point source over the object will be phase shifted to each other.

In Structured Illumination Microscopy (SIM) the object is modulated by a pattern. Usually the pattern is sinusoidal and created by a grid placed in a conjugated image plane. As the whole sample is illuminated the light used for structuring is coherent. By interference of the grid structure with object structures Moiré fringes are created that contain high frequency information that is downshifted to a lower frequency band. By shifting the grid a set of phase shifted images is created that is used to assign the frequencies back to their correct position during a deconvolution step. By rotation of the grid most of the object will be sampled.

In Airyscanning the object is illuminated by a point source which is moved over the sample. The signal is imaged on a detector array comprising several detector elements that have a fixed geometry to the optical axis and to each other. As the sample is scanned, each detector element will record the whole image. The images of the single detector elements will be phase shifted to each other. The contribution of each detector element is determined by a deconvolution step that reassigns the frequencies captured in the displaced elements to their correct positions. As illumination with the points source is sequential, the structuring light would be incoherent.

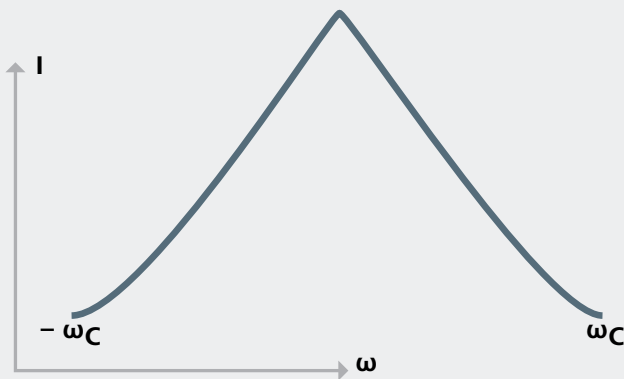
Box 9: Intensity distribution in the OTF

Figure B9 Optical transfer function. Normalized OTF amplitude corresponding to the modulation transfer function MTF in one transverse direction. The OTF drops to 0 at the cut-off frequency ω_c . Simulations done with $NA=1.44$; $\lambda=488$; $I_0=1$.

The optical transfer function (OTF) is the Fourier transform of the point spread function (PSF) and a complex valued function (equation 1). The relative contrast is given by the absolute value of OTF, which is commonly referred to as the modulation transfer function (MTF) (equation 2). The pattern translation is given by the phase transfer function (PhTF)

(equation 3), which is the complex argument function of the OTF. The MTF can be described by trigonometric functions (equation 4).

$$(1) \quad OTF(\omega) = MTF(\omega) * e^{i*PhTF(\omega)}$$

$$(2) \quad MTF(\omega) = |OTF(\omega)|$$

$$(3) \quad PhTF(\omega) = \arg(OTF(\omega))$$

$$(4a) \quad MTF(\omega) = I_0 \cdot \frac{2}{\pi} \cdot (\Phi(\omega) - \sin \Phi(\omega) \cdot \cos \Phi(\omega))$$

$$(4b) \quad \Phi(\omega) = \cos^{-1} \left(\frac{\omega}{\omega_c} \right)$$

$$(4c) \quad \omega_c = \frac{2 \cdot NA}{\lambda}$$

Parameters. ω : spatial frequency, ω_c : cut-off frequency, I_0 : amplitude, NA: numerical aperture; λ : wavelength



Carl Zeiss Microscopy GmbH
07745 Jena, Germany
microscopy@zeiss.com
www.zeiss.com/microscopy



We make it visible.